Overexpression of hsa_circ_0006470 inhibits the malignant behavior of gastric cancer cells *via* regulation of miR-1234/TP53I11 axis

Jinbi Xie,[1]* Yong Ning,[2]* Lihang Zhang,[1] Yuan Lin,[1] Runsheng Guo,[2] Shanjuan Wang[1]

[1]Department of Gastroenterology; [2]Department of General Surgery, Jiading District Central Hospital Affiliated Shanghai University of Medicine and Health Sciences, Shanghai, China
**These authors contributed equally to this work*

ABSTRACT

Gastric cancer (GC) is a subtype of a common malignant tumor found in the digestive system. Hsa_circ_0006470 is known to be closely associated with the development of GC. Nevertheless, the mechanism by which hsa_circ_0006470 regulates the tumorigenesis of GC has not been fully elucidated. To investigate the role of hsa_circ_0006470 in GC, its expression levels were assessed in GES-1, AGS, MKN45, and SNU5 cells by reverse transcription-quantitative PCR. Fluorescence *in situ* hybridization was used to evaluate the localization of hsa_circ_0006470 in AGS and MKN45 cells. In addition, cell counting kit-8 and 5-ethynyl-2'-deoxyuridine assays were performed to evaluate the viability and proliferation of GC cells, respectively. The dual-luciferase reporter assay was used to explore the interaction among hsa_circ_0006470, microRNA (miR)-1234, and TP53I11. The expression levels of TP53I11, Akt, p-Akt, forkhead box O1, and cyclin dependent kinase 2 in AGS cells were analyzed by Western blotting. The data indicated that hsa_circ_0006470 expression was downregulated in AGS cells. In addition, overexpression (OE) of hsa_circ_0006470 could inhibit the viability and proliferation of GC cells. Moreover, OE of hsa_circ_0006470 inhibited the migration of GC cells and induced G_1 cell cycle phase arrest. Moreover, miR-1234 was bound to hsa_circ_0006470 and TP53I11 was targeted by miR-1234. Furthermore, OE of hsa_circ_0006470 inhibited the tumorigenesis of GC *via* the regulation of the miR-1234/TP53I11 axis. In summary, the present study demonstrated that OE of hsa_circ_0006470 notably inhibited the tumorigenesis of GC by regulating the miR-1234/TP53I11 axis. Therefore, the present study may provide a theoretical basis for exploring novel therapeutic strategies for the treatment of GC.

Key words: Gastric cancer; hsa_circ_0006470; miR-1234; TP53I11; cell viability.

Correspondence: Runsheng Guo, Department of General Surgery, Shanghai Jiading District Central Hospital, 1 Chengbei Road, Jiading District, Shanghai, 201800 China. E-mail: guorunsheng2012@126.com

Key words: gastric cancer; hsa_circ_0006470; miR-1234; TP53I11; cell viability.

Contributions: SW, research supervision; JX, YN, SW, study design; JX, LZ, YL, experiments performing; RG, manuscript performing. All the authors have read and approved the final version of the manuscript and agreed to be accountable for all aspects of the work.

Conflict of interest: The authors declare that they have no competing interests, and all authors confirm accuracy.

Ethics approval: The Ethical Committee of Shanghai Jiading District Central Hospital approved this study (No. SHJDCH20220407).

Availability of data and materials: The datasets analyzed during the current study are available from the corresponding author on reasonable request.

Funding: This work was supported by Project of Jiading District Science and Technology Commission (JDKW-2019-w01).

Introduction

Gastric cancer (GC) is a subtype of a common malignant tumor found in the digestive system.[1] The main factors that induce GC are poor nutritional habits (long-term intake of preserved foods), *Helicobacter pylori* infection, chronic diseases and genetics.[2-4] Early-stage GC is mostly asymptomatic or presents with mild symptoms.[1] When the clinical symptoms are evident, the disease is already at an advanced stage.[1,5] Patients with advanced GC suffer from great physical and psychological pain.[6,7] The main treatment strategies for GC include drug and surgical treatments; however, the outcomes are not ideal.[1,8] Therefore, it is imperative to explore novel therapeutic strategies against GC.

Circular RNA (circRNA) is a subtype of closed circular RNA molecules formed by reverse splicing.[9,10] The characteristics of circRNA molecules include high stability, biological evolutionary conservation and tissue expression specificity.[11-13] It has been reported that circRNAs can exert various biological functions.[14,15] For example, they can be used as a "sponge" of microRNAs (miRs) or as a competitive endogenous RNA of miRs.[14,16] CircRNAs are differentially expressed in multiple tumors (GC, prostate cancer, and colorectal cancer).[15,17,18] Moreover, hsa_circ_0004872 significantly inhibits the growth of GC cells by regulating miR-224 expression.[19] In addition, overexpression (OE) of circCUL2 inhibits the malignant phenotype of cancer cells by targeting miR-142-3p.[20] Moreover, hsa_circ_0006470 expression was downregulated in GC.[21] Nevertheless, the mechanism by which hsa_circ_0006470 regulates the tumorigenesis of GC is still unclear.

Based on the aforementioned evidence, the present research study aimed to investigate the function of hsa_circ_0006470 in GC. This investigation can aid the exploration of novel therapeutic strategies against GC.

Materials and Methods

Cell culture

The human gastric epithelial cell line GES-1 was purchased from Beyotime Institute of Biotechnology (Suzhou, China). The GC cell lines AGS and SNU5 were obtained from ATCC. The GC cell line MKN45 was provided by Procell Life Science & Technology Co., Ltd. (Wuhan, China). GES-1, AGS, MKN45, and SNU5 cells were cultured in DMEM supplemented with 100 U/mL penicillin/streptomycin and 10% FBS at 37°C in the presence of 5% CO_2.

Reverse transcription-quantitative polymerase chain reaction (RT-qPCR)

The isolation of total RNA from GES-1, AGS, MKN45, or SNU5 cells was achieved with TRIzol® reagent (Takara Bio, Inc., Kusatsu, Japan). Subsequently, the RNA was converted into cDNA using EntiLink™ 1st Strand cDNA Synthesis Kit (Takara Bio, Inc.). The StepOne™ Real-Time PCR System (Applied Biosystems 7500) was used to perform quantitative PCR. The primer sequences used were as follows: β-actin, forward, 5'-GTCCACCGCAAATGCTTCTA-3', reverse, 5'-TGCTGTCACCTTCACCGTTC-3'; hsa-circ-0006470, forward, 5'-TTCGACTCATCATGGACTCCC-3', reverse, 5'-GACACAAAGAAGATGCGGTCC-3'; hsa-liner-0006470, forward, 5'-CTGCTAAGGAGGTGCTCAACG-3', reverse, 5'-CGTGTGCTGCTCAAACTTG-3'; TP53I11, forward, 5'-TGATGCGGTCTTTGATGGAG-3', reverse, 5'-CAGTGACCACCAAGAACTGGAC-3'. The expression levels of the genes of interest were normalized to those of β-actin. The data were analyzed using the $2^{-\Delta\Delta Cq}$ method.

Fluorescence *in situ* hybridization (FISH) analysis

FISH was applied to evaluate the localization of hsa_circ_0006470 in AGS and MKN45 cells. The same method was applied to identify the interaction of hsa_circ_0006470 and miR-1234 in AGS cells. The fluorescence-labeled oligonucleotide probes for hsa_circ_0006470 and miR-1234 were obtained from Guangzhou RiboBio Co., Ltd. (Guangzhou, China). Subsequently, AGS and MKN45 cells were incubated with the mixture containing the probes, and FITC-Avidin was used to stain the probe. In addition, the nuclei were stained using 4',6-diamidino-2-phenylindole (DAPI). Subsequently, the localization of hsa_circ_0006470 in AGS and MKN45 cells was investigated using a fluorescence microscope (BX51TF, Olympus Corporation, Tokyo, Japan). The filter sets were as follows: blue excitation: 420~485 nm; green excitation: 460~550 nm; red excitation: 420~490 nm.

Cell transfection

AGS and MKN45 cells were transfected with a pcDNA3.1 vector designed to induce OE of hsa_circ_0006470 (Guangzhou RiboBio Co., Ltd.) or a pcDNA3.1 control vector (pcDNA3.1-ctrl, Guangzhou RiboBio Co., Ltd.) using Lipofectamine™ 2000 (Invitrogen; Thermo Fisher Scientific, Inc., Waltham, MA, USA) according to the manufacturer's protocol. AGS cells were transfected with miR-1234 mimics or miR-1234 mimics-control (mimics-ctrl, Guangzhou RiboBio Co., Ltd.) using Lipofectamine™ 2000. AGS cells were transfected with small interfering RNA (siRNA) against TP53I11 (TP53I11 siRNA1, TP53I11 siRNA2, TP53I11 siRNA3 or siRNA-control (siRNA-ctrl) (Guangzhou RiboBio Co., Ltd.) using Lipofectamine™ 2000. The sequences used for TP53I11 siRNAs and siRNA-ctrl were as follows: TP53I11 siRNA1: 5'-AGCAGTCAGTAGTTGGTCCTTTG-3'; TP53I11 siRNA2: 5'-CATCATCCCTGCCTCTACTGG-3'; TP53I11 siRNA3: 5'-CCATCAGTCCCGTCTTGAAAC-3'; siRNA-ctrl: 5'-GTGGGTGTCGCTGTTGAAGTC-3'.

Cell counting kit-8 (CCK-8) assay

CCK-8 was obtained from Beyotime Institute of Biotechnology. The cells were maintained in 96-well plates. Subsequently, AGS and MKN45 cells were incubated with 10 µL CCK-8 solution (Beyotime Institute of Biotechnology) at 37°C for 2 h following treatment. Subsequently, the viability of AGS and MKN45 cells was detected at 0, 12, 24, and 72 h using a microplate reader (Bio-Rad Laboratories, Inc., Hercules, CA, USA).

5-ethynyl-2'-deoxyuridine (EdU) staining

An EdU detection kit was obtained from Guangzhou RiboBio Co., Ltd. Following treatment, AGS and MKN45 cells were labeled with 100 µL 5-Ethynyl-2'- deoxyuridine (50 µM) for 1 h. The cells were washed with PBS twice for 5 min and incubated with 100 µL DAPI (1 µg/mL). Subsequently, the proliferation of AGS and MKN45 cells was detected using a fluorescence microscope (BX51TF, Olympus Corporation). Meanwhile, Apollo 567 was used to label the fluorochrome. The filter sets were as follows: blue excitation: 420~485 nm; red excitation: 420~490 nm.

Transwell assay

DMEM with 10% serum was added to the basolateral chamber. Moreover, AGS and MKN45 cells were cultured in the apical chamber with 200 µL serum-free DMEM. Following incubation for 24 h, the medium in the basolateral chamber was removed and

the cells were removed with PBS. Subsequently, the cells were fixed with paraformaldehyde for 20 min and stained with 0.1% crystal violet for 10 min. Finally, the migrated cells were detected using an optical microscope (BX53, Olympus Corporation).

Cell cycle distribution assay

AGS and MKN45 cells were collected using 0.25% trypsin. Subsequently, they were fixed with 70% ethanol and treated with propidium iodide (2 μg/mL)/RNase (10 mg/mL) staining buffer for 15 min in the dark at 4°C. The distribution of the cells was analyzed using a flow cytometer (FACScan™, BD Biosciences, Franklin Lakes, NJ, USA). The percentage of cell cycle phases was quantified using FlowJo software (FlowJo LLC, Ashland, OR, USA).[22] Three measurement series per sample were recorded, and three replicates were performed in each group.

Dual-luciferase reporter assay

hsa_circ_0006470 wild-type/mutated-type (WT/MT) or TP53I11 (WT/MT) were synthesized by Sangon Biotech (Shanghai, China). The synthetic sequences were inserted into the pmiR-RB-REPORT™ vector. Subsequently, AGS cells were transfected with the recombinant vector of WT/MT containing miR-1234 mimics or miR-1234 mimics-ctrl using Lipofectamine™ 2000. The luciferase activity of AGS cells was assessed using a dual-luciferase reporter assay system.

Western blot assay

AGS cells were lysed and the total protein was extracted using a protein lysis buffer. Subsequently, the protein concentration was determined by a bicinchoninic acid protein assay kit (Beyotime Institute of Biotechnology). The protein samples were separated by PAGE using 10% SDS gels (30 μg per lane). Subsequently, the proteins were transferred to polyvinylidene fluoride membranes (Beyotime Institute of Biotechnology). The following primary antibodies were used: TP53I11 (1:1,000, ab234860), Akt (1:1,000, ab8805), phosphorylated (p)-Akt (1:1,000, ab38449), forkhead box O (FOXO) 1 (1:1,000, ab179450), cyclin-dependent kinase (CDK) 2 (1:1,000, ab32147), β-actin (1:1,000, ab8226). A horseradish peroxidase-labeled secondary antibody (1:5,000, ab7090) was also used for western blotting. All antibodies were obtained from Abcam (Cambridge, UK). Finally, an ECL kit was employed to detect the protein expression. The expression levels of these proteins were normalized to those of β-actin.

Statistical analysis

The data were analyzed by GraphPad Prism. All data are presented as the mean ± standard deviation. The differences were assessed by one-way analysis of variance (ANOVA) and Tukey's tests. A p-value <0.05 was considered to indicate a statistically significant difference.

Results

hsa_circ_0006470 is expressed at low levels in AGS cells

It has been reported that the expression hsa_circ_0006470 is downregulated in GC.[21] To confirm the role of hsa_circ_0006470 in GC cells, RT-qPCR was performed. As shown in Figure 1A, the levels of hsa_circ_0006470 in GC cells were lower compared with those of GES-1 cells. Since the expression levels of hsa_circ_0006470 were lower in AGS and MKN45 cells compared with those of SNU5 cells, these two cell lines were selected for subsequent experiments (Figure 1A). The results of FISH analysis indicated that hsa_circ_0006470 was mainly localized in the cytoplasm of GC cells (Figure 1B). Furthermore, RNase R did not

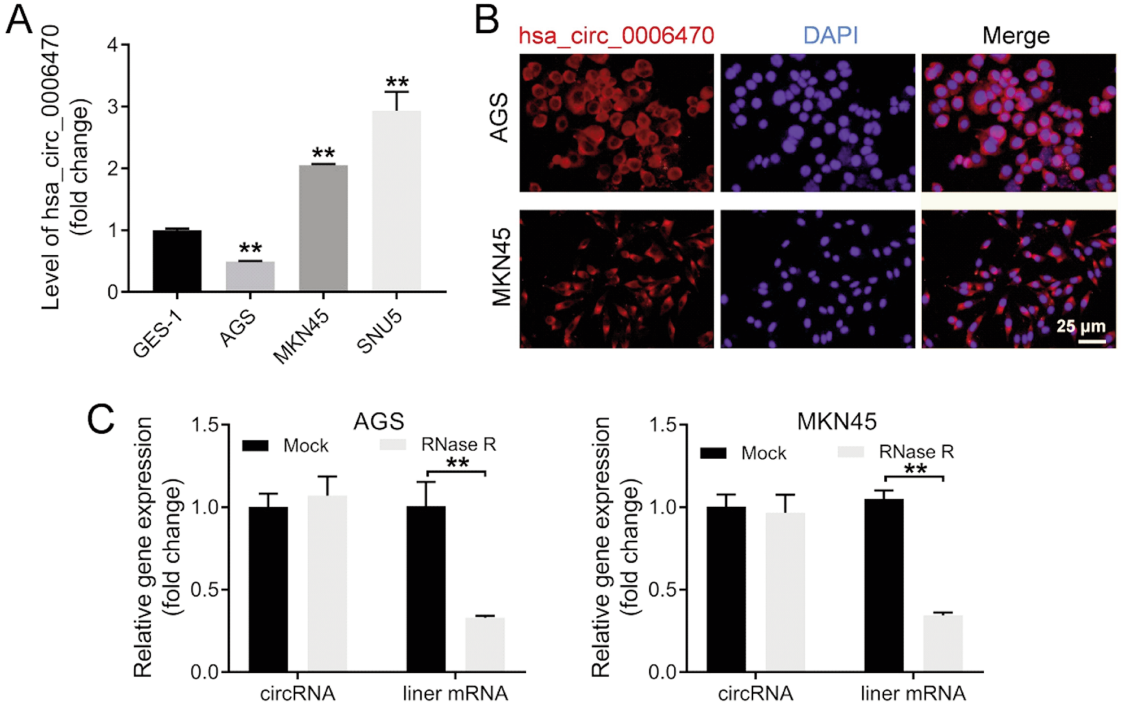

Figure 1. Hsa_circ_0006470 is downregulated in AGS cells. A) RT-qPCR was performed to evaluate the expression of hsa_circ_0006470 in GES-1, AGS, MKN45 and SNU5 cells. B) FISH was used to evaluate the localization of hsa_circ_0006470 in AGS and MKN45 cells. C) RT-qPCR was performed to confirm the level of hsa_circ_0006470 in AGS and MKN45 cells.p<0.01 compared with control group.**

affect the expression levels of hsa_circ_0006470 in AGS and MKN45 cells, while it significantly inhibited the expression levels of the linear mRNA molecule (Figure 1C). These data suggested that hsa_circ_0006470 exhibited a closed cyclic structure. Moreover, the data suggested that hsa_circ_0006470 expression was downregulated in AGS cells.

Overexpression of hsa_circ_0006470 inhibits the viability and proliferation of GC cells

To explore the function of hsa_circ_0006470 in GC cells, they were transfected with a hsa_circ_0006470 OE vector. The results indicated that hsa_circ_0006470 OE caused a marked upregulation in the expression levels of hsa_circ_0006470 in GC cells (Figure 2A). In addition, hsa_circ_0006470 OE suppressed the viability of GC cells (Figure 2B). hsa_circ_0006470 upregulation inhibited the proliferation of GC cells (Figure 2 C,D). In summary, OE of hsa_circ_0006470 notably inhibited the proliferation of GC cells.

Overexpression of hsa_circ_0006470 inhibits the migration of GC cells

In order to explore the effects of hsa_circ_0006470 on the migration of GC cells, a Transwell assay was performed. As shown in Figure 3 A,B, pcDNA3.1-hsa_circ_0006470 decreased the migration of GC cells. OE of hsa_circ_0006470 significantly inhibited the migration of GC cells.

Overexpression of hsa_circ_0006470 induces G1 phase arrest of GC cells

In order to evaluate the effects of hsa_circ_0006470 on the cell cycle distribution, flow cytometry was performed. As demonstrated in Figure 4 A,B, hsa_circ_0006470 OE caused a dramatic induction of G0-G1 phase arrest in GC cells.

hsa_circ_0006470 is bound to miR-1234

In order to identify the downstream miRs of hsa_circ_0006470 involved in the development of GC, the circular RNA interactome (https://circinteractome.nia.nih.gov/api/v2/mirnasearch?circular_rna_query=hsa_circ_0006470&mirna_query=hsa-miR-1234&submit=miRNA+Target+Search) was used. The results indicated that hsa_circ_0006470 could bind to miR-1234 in GC cells (Figure 5A), and miR-1234 was shown to play a vital part in the oncogenesis of GC.[23] Therefore, miR-1234 was selected in the present study. In addition, miR-1234 mimics significantly decreased the luciferase activity of WT-hsa_circ_0006470, while it did not affect the luciferase activity in MT-hsa_circ_0006470 (Figure 5B). hsa_circ_0006470 was found to be co-localized with miR-1234 in AGS cells (Figure 5C).

To further explore the target of miR-1234, TargetScan was used. It was predicted that TP53I11 may be the downstream mRNA of miR-1234 (Figure 5D); moreover, TP53I11 has been shown to be a vital mediator of cell cycle progression.[24] Therefore, TP53I11 was selected in the current study. In addition, miR-1234 mimics notably inhibited the luciferase activity of WT-TP53I11, whereas it had very limited effects on the luciferase activity of MT-TP53I11 (Figure 5E). Moreover, hsa_circ_0006470 OE significantly increased the levels of TP53I11 in AGS cells (Figure 5 F,G). Taken together, the data indicated that hsa_circ_0006470 was bound to miR-1234 and TP53I11 was directly targeted by miR-1234.

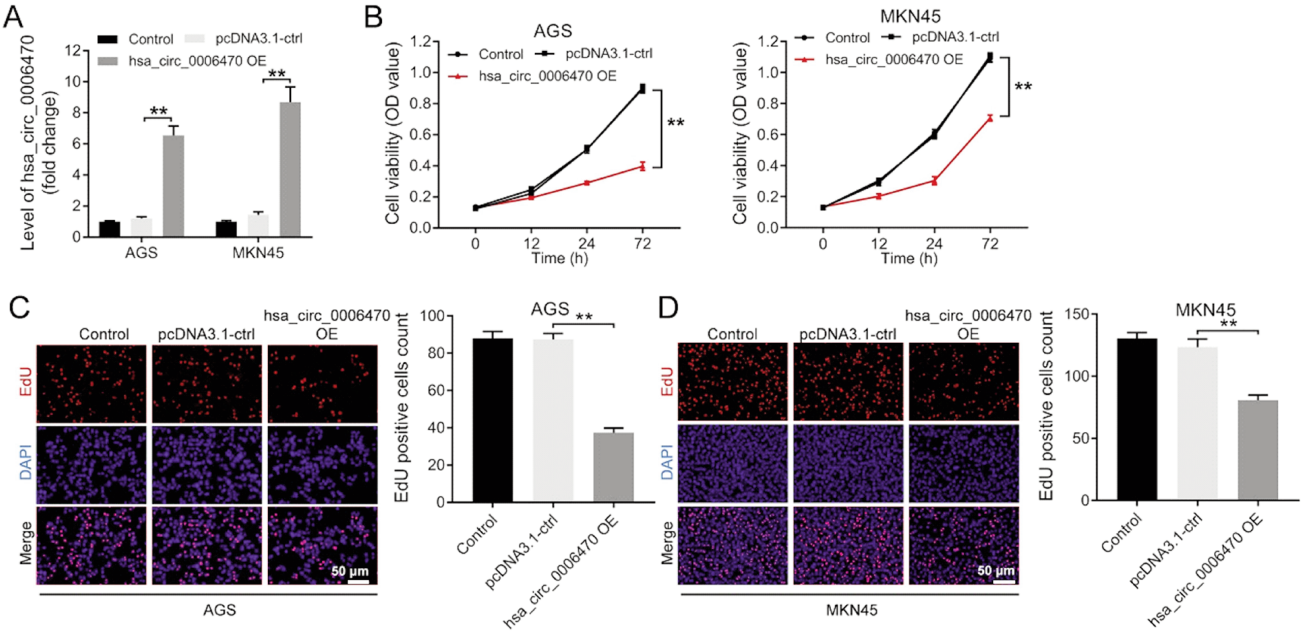

Figure 2. Overexpression of hsa_circ_0006470 inhibits the viability and proliferation of GC cells. AGS or MKN45 cells were transfected with pcDNA3.1- hsa_circ_0006470 OE or pcDNA3.1-ctrl. A) RT-qPCR was used to evaluate the expression of hsa_circ_0006470 in AGS and MKN45 cells. B) The viability of AGS and MKN45 cells was tested by CCK8 assay. C,D) The proliferation of AGS and MKN45 cells was evaluated by EdU staining. **p<0.01 compared with control group.

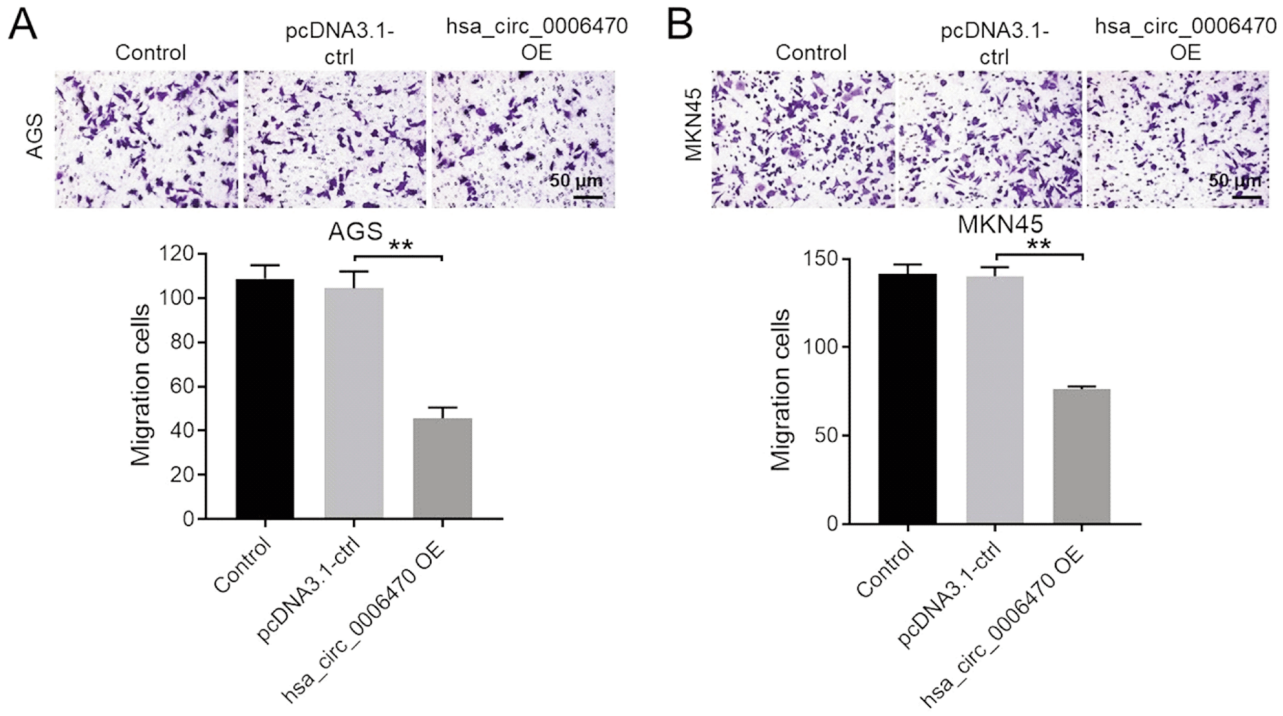

Figure 3. Overexpression of hsa_circ_0006470 inhibits the migration of GC cells. Transwell assay was used to evaluate the migration of GC cells. **p<0.01 compared with control group.

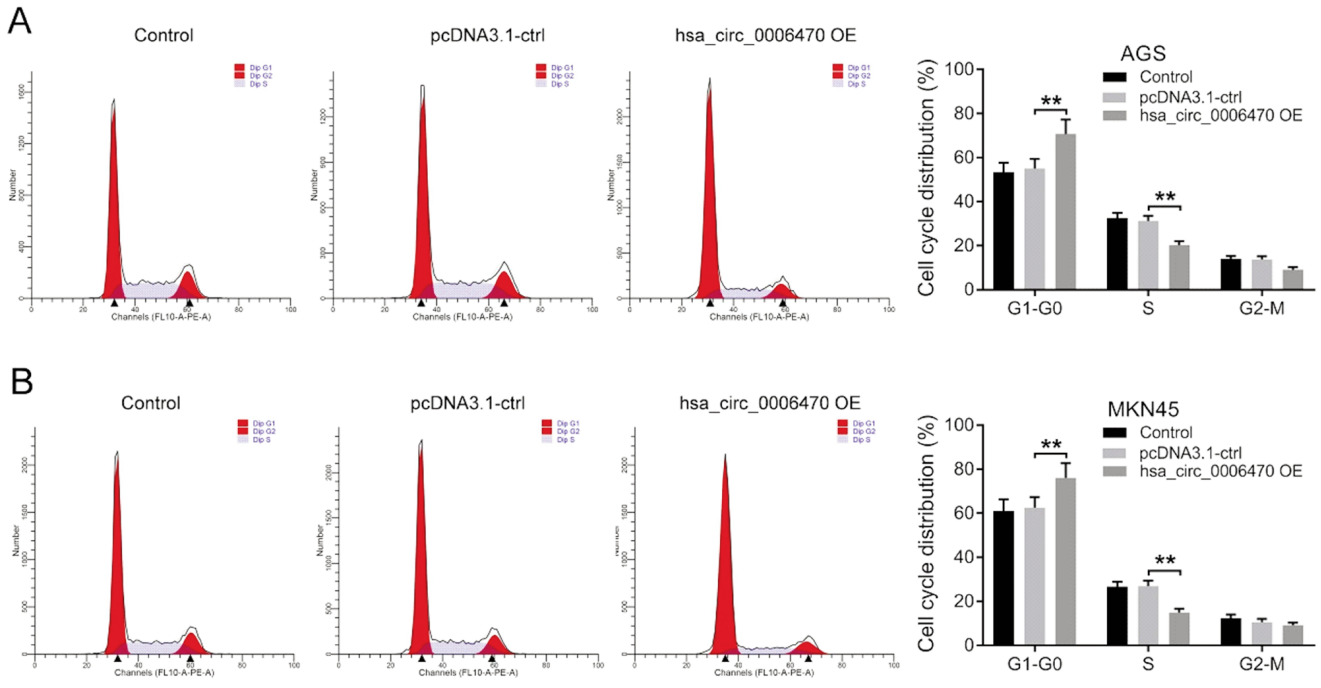

Figure 4. Overexpression of hsa_circ_0006470 induces G_1 phase arrest in GC cells. The cell cycle distribution was tested by low cytometry. **p<0.01 compared with control group.

Overexpression of hsa_circ_0006470 inhibits the proliferation of GC cells by regulating the miR-1234/TP53I11 axis

To further investigate the mechanism by which hsa_circ_0006470 regulates the tumorigenesis of GC, GC cells were treated with TP53I11 siRNA. The transfection efficiency was investigated. Transfection of the cells with TP53I11 siRNA notably decreased the expression levels of TP53I11 in AGS cells (Figure 6A). Since GC cells were more sensitive to the effects of TP53I11 siRNA1, the latter was selected for subsequent analysis (Figure 6A). In addition, hsa_circ_0006470 OE notably inhibited the viability of AGS cells, while this phenomenon was reversed by TP53I11 siRNA1 (Figure 6B). Moreover, upregulation of hsa_circ_0006470 expression significantly increased the expression levels of TP53I11 and FOXO1 and inhibited the expression levels of p-Akt and CDK2 in AGS cells; however, these phenomena were notably reversed in the presence of TP53I11 siRNA1 (Figure 6 C-G). In conclusion, OE of hsa_circ_0006470 notably suppressed the viability of GC cells by regulating the miR-1234/TP53I11 axis.

Discussion

GC seriously affects the physical and mental health of patients.[25] The expression levels of specific circRNAs are closely associated with the neoplastic transformation of GC cells.[26] In addition, it has been reported that hsa_circ_0006470 is involved in the progression of GC. For example, Cui et al found that hsa_circ_0006470 expression was significantly upregulated in GC cells and that it could regulate the proliferation, migration, and invasion of GC cells by binding to miR-27b-3p;[27] Yao *et al*. indi-

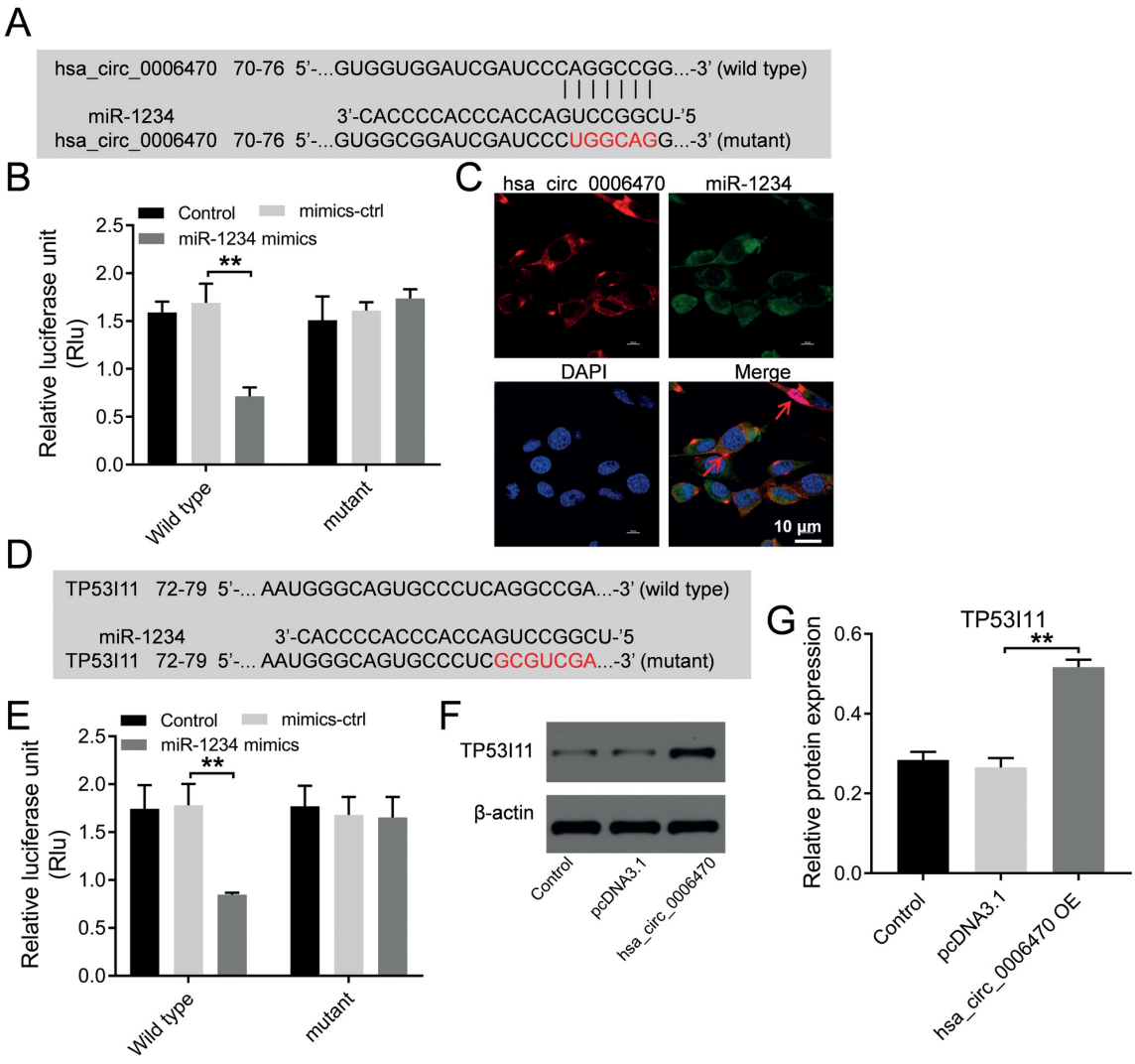

Figure 5. miR-1234 is sponged by hsa_circ_0006470, and TP53I11 is targeted by miR-1234. A) Circular RNA interactome was used to predict the binding sites between miR-1234 and hsa_circ_0006470. B) The relative luciferase activity in WT/MT-hsa_circ_0006470 was measured by dual luciferase reporter assay. C) The co-localization between hsa_circ_0006470 and miR-1234 in GC cells was explored by FISH. D) Target scan was performed to predict the targets of miR-1234. E) The relative luciferase activity in WT/MT-TP53I11 was tested by dual luciferase reporter assay. F,G) Western blot was used to evaluate the level of TP53I11 in AGS cells. **p<0.01 compared with control group.

cated that the downregulation of the expression of hsa_circ_0006470 could predict tumor invasion of GC.[21] In the current study, the data indicated that hsa_circ_0006470 OE could inhibit the malignant phenotype of GC cells and that hsa_circ_0006470 could bind to miR-1234. The current study explored the interaction between hsa_circ_0006470 and miR-1234 with regard to GC progression. Therefore, the data presented may provide novel evidence that can be used to investigate further the mechanisms underlying the function of circRNAs in GC.

circRNAs can bind to certain miRs during the progression of GC.[14,16] For example, OE of circ_SH3KBP1 binding protein 1 promoted the angiogenesis of GC cells by sponging miR-582-3p.[28] Moreover, OE of circ-coiled-coil domain containing 9 suppressed the proliferation of GC cells by targeting miR-6792-3p. Similarly, miR-1234 was targeted by hsa_circ_0006470 in the present study. miR-6792-3p was verified to be a suppressor of cancer progression.[29] Therefore, the similar function between miR-1234 and miR-6792-3p in cancer may be used to explain the similar data presented between the current and previous research studies. In addition, OE of hsa_circ_0006470 induced cell cycle arrest of GC. Wang *et al.* indicated that TP53I11 is a cell cycle-related protein.[24] Therefore, it may be suggested that OE of hsa_circ_0006470 inhibits the proliferation of GC cells by regulating the miR-1234/TP53I11 axis.

In addition, downregulation of TP53I11 expression promotes the AKT pathway in MCF10A cells.[30] In the current study, upregulation of hsa_circ_0006470 expression significantly increased the expression levels of TP53I11, FOXO and inhibited the expression levels of p-Akt and CDK2 in AGS cells. The data reported in the present study were similar to those of previous reports, suggesting that TP53I11 could regulate the expression of AKT.

Based on the aforementioned evidence, the novelty of the current study was as follows: i) The interaction between hsa_circ_0006470 and miR-1234 with regard to the progression of GC was explored for the first time; ii) the downstream mRNA of miR-1234 was investigated for the first time.

In conclusion, OE of hsa_circ_0006470 notably inhibited the tumorigenesis of GC cells by regulating the miR-1234/TP53I11 axis. The findings may shed light on the discovery of novel therapeutic strategies against GC.

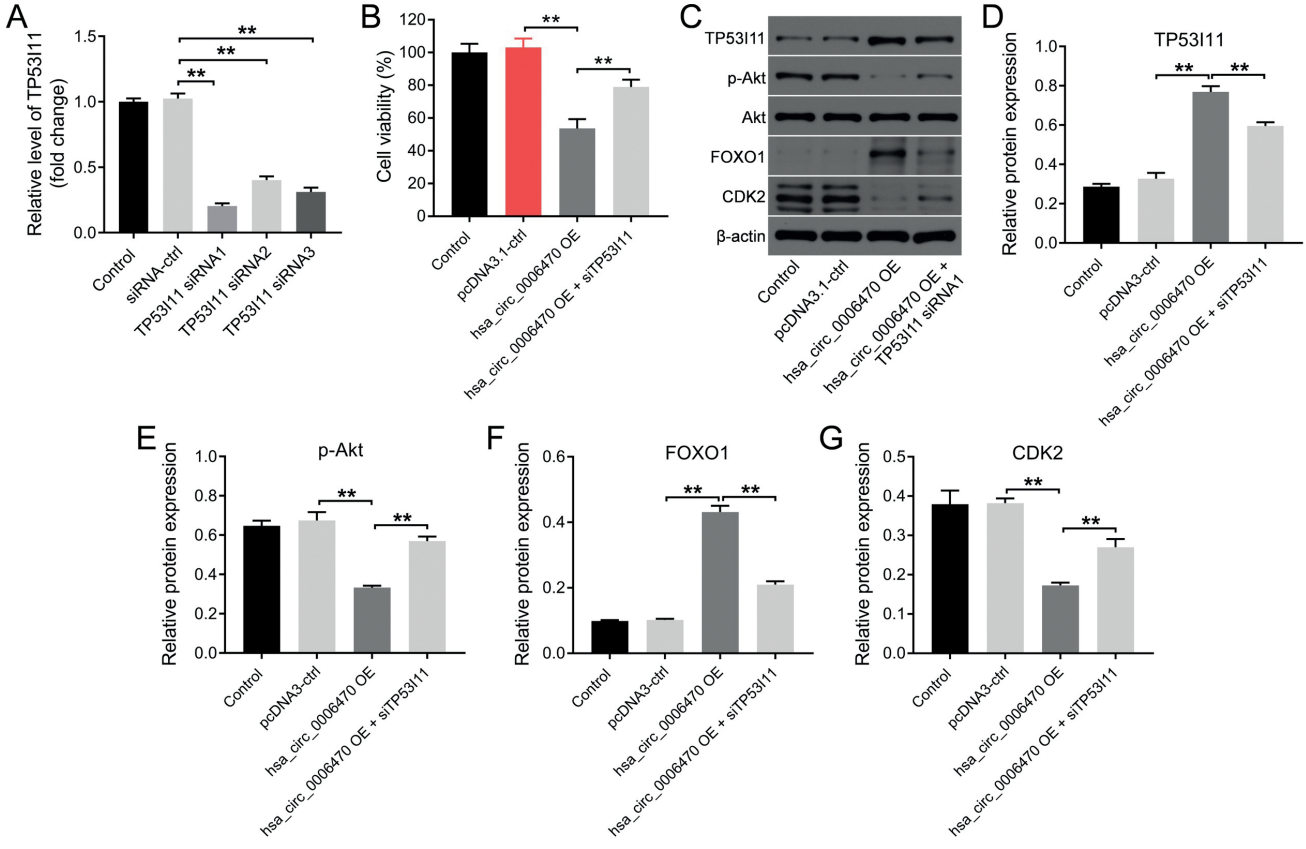

Figure 6. Overexpression of hsa_circ_0006470 inhibits the viability of GC cells *via* regulating miR-1234/TP53I11 axis and inhibiting Akt/FOXO1/CDK2 pathway. AGS cells were transfected withTP53I11 siRNA1, TP53I11 siRNA2, TP53I11 siRNA3 orTP53I11 siRNA-control. A) RT-qPCR was used to evaluate the level of TP53I11 in AGS cells. B) The viability of GC cells was assessed by CCK8 assay. C-G) Western blot assay was performed to evaluate the level of TP53I11, Akt, p-Akt, FOXO1 and CDK2 in AGS cells.p<0.01 compared with control group.**

References

1. Song Z, Wu Y, Yang J, Yang D, Fang X. Progress in the treatment of advanced gastric cancer. Tumour Biol 2017;39: 1010428317714626.
2. Somi MH, Mousavi SM, Naghashi S, Faramarzi E, Jafarabadi MA, Ghojazade M, et al. Is there any relationship between food habits in the last two decades and gastric cancer in North-Western Iran? Asian Pac J Cancer Prev 2015;16:283-90.
3. Amieva M, Peek RM, Jr. Pathobiology of Helicobacter pylori-induced gastric cancer. Gastroenterology 2016;150:64-78.
4. Karimi P, Islami F, Anandasabapathy S, Freedman ND, Kamangar F. Gastric cancer: descriptive epidemiology, risk factors, screening, and prevention. Cancer Epidemiol Biomarkers Prev 2014;23:700-13.
5. Tan Z. Recent advances in the surgical treatment of advanced gastric cancer: A review. Med Sci Monit 2019;25:3537-41.
6. Religioni U, Czerw A, Badowska-Kozakiewicz AM, Deptała A. Assessment of pain, acceptance of illness, adjustment to life, and strategies of coping with illness among patients with gastric cancer. J Cancer Educ 2020;35:724-30.
7. Ma X, Sun S, Zhao Y, Wang X, Meng W, Pang Z, et al. Impact of pain care and hospice care on quality of life in patients with advanced gastric cancer. Am J Transl Res 2021;13:8235-40.
8. Smyth EC, Nilsson M, Grabsch HI, van Grieken NC, Lordick F. Gastric cancer. Lancet 2020;396:635-48.
9. Zhou WY, Cai ZR, Liu J, Wang DS, Ju HQ, Xu RH. Circular RNA: metabolism, functions and interactions with proteins. Mol Cancer 2020;19:172.
10. Li X, Li C, Liu Z, Ni W, Yao R, Xu Y, et al. Circular RNA circFoxO3 inhibits myoblast cells differentiation. Cells 2019;8:616. Retracted Article in: Cells 2020;9:2504.
11. Vo JN, Cieslik M, Zhang Y, Shukla S, Xiao L, Zhang Y, et al. The landscape of circular RNA in cancer. Cel. 2019;176:869-81.e13.
12. Zhou Z, Sun B, Huang S, Zhao L. Roles of circular RNAs in immune regulation and autoimmune diseases. Cell Death Dis 2019;10:503.
13. Kristensen LS, Andersen MS, Stagsted LVW, Ebbesen KK, Hansen TB, Kjems J. The biogenesis, biology and characterization of circular RNAs. Nat Rev Genet 2019;20:675-91.
14. Hong X, Liu N, Liang Y, He Q, Yang X, Lei Y, et al. Circular RNA CRIM1 functions as a ceRNA to promote nasopharyngeal carcinoma metastasis and docetaxel chemoresistance through upregulating FOXQ1. Mol Cancer 2020;19:33.
15. Zhang X, Wang S, Wang H, Cao J, Huang X, Chen Z, et al. Circular RNA circNRIP1 acts as a microRNA-149-5p sponge to promote gastric cancer progression via the AKT1/mTOR pathway. Mol Cancer 2019;18:20.
16. Lu Q, Liu T, Feng H, Yang R, Zhao X, Chen W, et al. Circular RNA circSLC8A1 acts as a sponge of miR-130b/miR-494 in suppressing bladder cancer progression via regulating PTEN. Mol Cancer.2019;18:111.
17. Shen Z, Zhou L, Zhang C, Xu J. Reduction of circular RNA Foxo3 promotes prostate cancer progression and chemoresistance to docetaxel. Cancer Lett 2020;468:88-101.
18. Chen LY, Wang L, Ren YX, Pang Z, Liu Y, Sun XD, et al. The circular RNA circ-ERBIN promotes growth and metastasis of colorectal cancer by miR-125a-5p and miR-138-5p/4EBP-1 mediated cap-independent HIF-1α translation. Mol Cancer 2020;19:164.
19. Ma C, Wang X, Yang F, Zang Y, Liu J, Wang X, et al. Circular RNA hsa_circ_0004872 inhibits gastric cancer progression via the miR-224/Smad4/ADAR1 successive regulatory circuit. Mol Cancer 2020;19:157.
20. Peng L, Sang H, Wei S, Li Y, Jin D, Zhu X, et al. circCUL2 regulates gastric cancer malignant transformation and cisplatin resistance by modulating autophagy activation via miR-142-3p/ROCK2. Mol Cancer 2020;19:156.
21. Yao L, Xie Y. Down-regulation of hsa_circ_0006470 predicts tumor invasion: A new biomarker of gastric cancer. J Clin Lab Ana. 2021;35:e23879.
22. Wong LS, Wei L, Wang GC, Law CT, Tsang HC, Chin WC, et al. In vivo genome-wide CRISPR activation screening identifies functionally important long non-coding RNAs in hepatocellular carcinoma. Cell Mol Gastroenterol Hepatol 2022. Online Ahead of Print.
23. Dong L, Deng J, Sun ZM, Pan AP, Xiang XJ, Zhang L, et al. Interference with the β-catenin gene in gastric cancer induces changes to the miRNA expression profile. Tumour Biol 2015;36:6973-83.
24. Wang L, Huang J, Jiang M, Lin H. Tissue-specific transplantation antigen P35B (TSTA3) immune response-mediated metabolism coupling cell cycle to postreplication repair network in no-tumor hepatitis/cirrhotic tissues (HBV or HCV infection) by biocomputation. Immunol Res 2012;52:258-68.
25. Guggenheim DE, Shah MA. Gastric cancer epidemiology and risk factors. J Surg Oncol 2013;107:230-6.
26. Li R, Jiang J, Shi H, Qian H, Zhang X, Xu W. CircRNA: a rising star in gastric cancer. Cell Mol Life Sci 2020;77:1661-80.
27. Cui Y, Cao J, Huang S, Ye J, Huang H, Liao D, et al. circRNA_0006470 promotes the proliferation and migration of gastric cancer cells by functioning as a sponge of miR-27b-3p. Neoplasma 2021;68:1245-56.
28. Xie M, Yu T, Jing X, Ma L, Fan Y, Yang F, et al. Exosomal circSHKBP1 promotes gastric cancer progression via regulating the miR-582-3p/HUR/VEGF axis and suppressing HSP90 degradation. Mol Cancer 2020;19:112.
29. Luo Z, Rong Z, Zhang J, Zhu Z, Yu Z, Li T, et al. Circular RNA circCCDC9 acts as a miR-6792-3p sponge to suppress the progression of gastric cancer through regulating CAV1 expression. Mol Cancer 2020;19:86.
30. Xiao T, Xu Z, Zhou Y, Zhang H, Geng J, Liang Y, et al. Loss of TP53I11 enhances the extracellular matrix-independent survival by promoting activation of AMPK. IUBMB Life 2019;71:183-91.

Received for publication: 4 July 2022. Accepted for publication: 9 September 2022.

European Journal of Histochemistry 2022; 66:3477
doi:10.4081/ejh.2022.3477